ARS ADVANCED ROBOTIC SYSTEMS INTERNATIONAL

Bio-inspired Miniature Suction Cups Actuated by Shape Memory Alloy

Hu Bing-shan[1], Wang Li-wen[2], Fu Zhuang[1] and Zhao Yan-zheng[1]
[1]Research Institute of Robotics, School of Mechanical Engineering, Shanghai Jiao Tong University, 800 Dongchuan road, Shanghai 200240, P.R. of China
[2]The Research Base of Ground Support Equipment, Civil Aviation University of China, 100 Xunhai Road, Tianjin 300300, P.R. of China
Corresponding author E-mail: yzh-zhao@sjtu.edu.cn

Abstract: *Wall climbing robots using negative pressure suction always employ air pumps which have great noise and large volume. Two prototypes of bio-inspired miniature suction cup actuated by shape memory alloy (SMA) are designed based on studying characteristics of biologic suction apparatuses, and the suction cups in this paper can be used as adhesion mechanisms for miniature wall climbing robots without air pumps. The first prototype with a two-way shape memory effect (TWSME) extension TiNi spring imitates the piston structure of the stalked sucker; the second one actuated by a one way SMA actuator with a bias has a basic structure of stiff margin, guiding element, leader and elastic element. Analytical model of the second prototype is founded considering the constitutive model of the SMA actuator, the deflection of the thin elastic plate under compound load and the thermo-dynamic model of the sealed air cavity. Experiments are done to test their suction characteristics, and the analytical model of the second prototype is simulated on Matlab/simulink platform and validated by experiments.*
Keywords: *Suction cup; bio-inspired; SMA; miniature; wall climbing robot*

1. Introduction

Reliable suction on vertical wall is one of key technologies of wall climbing robots. Traditional suction methods include negative pressure and magnetic force, but magnetic force is only suitable for surfaces made of magnetic materials (Xu, Z.L., 2006). Negative pressure suction is applied broadly because of its large suction force and universal to all wall materials (Dean, M., 2005, Zhao, Y.Z., 2004). Nowadays, wall climbing robots using negative pressure suction always use air pumps, which has a large noise, and too big to be used in miniature robot. To overcome these disadvantages, a robot named Dexter who gets suction force by pressing passive suction cups to wall using a motor has been designed (Werner, B., 2005), and a vibrating suction method which uses a motor vibrated in high-frequency to press suction cups continuously to get a steady negative pressure is also invented (Zhu, T., 2006).

In nature, lots of small animals exhibit wall climbing ability and they attach or detach to wall freely just consuming little of power. Strategies adopted in nature to perform wall climbing rely on a wide variety of ingenious mechanisms. For example, octopus and leech use suckers to generate negative pressure to anchor their bodies to the substratum (William, M.K., 2002, Gray, J., 1938). Geckos employ large numbers of very fine hairs that achieve adhesion via van der Waals force (Autumn, K., 2002). Tree frogs and aphids employ wet adhesion (Persson, B.N.J., 2007, Dixon, A.F.G., 1990). Some other insects, for example, arthropods and reptiles employ small spines to climb hard vertical surfaces (Dai, Z.D., 2002).

Comparing with the method of generating negative pressure using motors mentioned before, biologic suction apparatus are obviously more convenient and agile, so imitating principles of animals' attachment to wall, and investigating design methods of bio-inspired adhesion mechanism have great value. Now there are several researchers working on synthetic versions of adhesion mechanisms. A mechanical snail, which can climb a vertical wall on a layer non-newtonian fluid, has been developed (Chan, B., 2007). Two nanomolding fabrication techniques are proposed to fabricate synthetic gecko foot-hairs (Sitti, M., 2003). A new approach for climbing hard vertical surfaces with compliant microspine arrays inspired by mechanisms observed in some climbing insects and spiders also has been designed (Asbeck, A.T., 2006).

Until now, a few literatures about bio-inspired miniature suction mechanisms actuated by muscle-like actuators are reported. There is an adhesion mechanism imitating tapeworm for gastrointestinal tract, which contains micro hooks and a suction cup actuated by ionic polymer metal composites (IPMC), but the suction cup is just as an assistant for micro hooks (Menciassi, A., 2003). A simulation study on octopus-inspired artificial suckers is also implemented, which can serve as a base for design of artificial suckers (Grasso, W.F., 2007).

Based on studying characteristics of biologic suction apparatus, two prototypes of bio-inspired miniature

International Journal of Advanced Robotic Systems, Vol. 6, No. 3 (2009)
ISSN 1729-8806, pp. 151-160

suction cup actuated by SMA are designed in this paper. and the paper is organized as follows: Section 2 discusses characteristics of biologic suction apparatus and artificial actuators for the bio-inspired suction cup. Section 3 presents the mechanism design of the two prototypes. Analytical model of the prototype 2 is illustrated in section 4, and section 5 is about experiments. Conclusions and future work are given in section 6.

2. Biological inspiration

2.1. Characteristics of biologic suction apparatus

There are lots of animals with negative pressure suction ability, and usually they have suckers which are easy to deform (Fig.1). For example, some animals live in water: cephalopod (Smith, A.M., 1996), echeneid fish (Fulcher, B. A., 2006), limpet (Ellem, K.G., 2002), octopus and leech mentioned before, and so on. Besides animals in water, a kind of disk-winged bat living on land also has suction cups (Riskin, D.K., 2001).

Because of special structures of biologic suckers, their suction force are immense. It has been reported that suction force of a limpets can reach 25N, which weight less than 25g (Ellem, K.G., 2002). When biologic suckers suck a substratum, the absence of any pump like apparatus is obvious, so perfect sealing is necessary to maintain negative pressure especially when the substratum is rough. Biologic suckers structure are various, but it is reported that they usually are plates or hemispheres with elastic edges (Nachtigall, W., 2005). When contacting with a rough substratum, the elastic edge makes a negative copy of the rough host substratum, so compliant sealing is achieved (Bandyopadhyay, P.R., 2008). There are also some other special structures on elastic edge. Scanning electron micrography of suckers of octopus shows that the elastic edge composes of radial grooves, ridges and a rim of loose material. Such design should allow the elastic edge to expand and contract without losing any contact to ensure sealing (William, M.K., 2002). Some biologic suckers have stiff margins or reinforcing rings upon elastic edges to prevent elastic edges' collapse when suck (Nachtigall, W., 2005). Many near shore squids have stalked suckers which are basically a cylinder and piston design. The farther piston is pulled, the greater the negative pressure produced, and this kind of sucker may be amenable to engineering development (Bandyopadhyay, P.R., 2008, Walker, I.D., 2005).

Fig 1. Suckers of an octopus

Based on the above analysis, the bio-inspired suction cup should have the following structures: First it has a shape of plate or hemisphere with an elastic edge which can conform closely to substratum to ensure sealing. Second, because the attachment depends upon the creation of a reduced pressure in the sealed cavity between suction cup and substratum, artificial actuator must be powerful enough to exert force to increase the volume of the sealed cavity. Lastly, stiff margins or reinforcing rings are essential for preventing collapse during suction.

2.2. SMA actuator

The largest obstacle of designing a bio-inspired suction cup has been lack of engineered muscle-like actuators (William, M.K., 2002). The actuator should have output force and displacement large enough to generate negative pressure. The actuator also should have appropriate actuating frequency and energy density. Now none of artificial muscles can imitate muscle perfectly. IPMC and electro active polymer (EAP) have been proposed as the actuator of the bio-inspired suction cup (Menciassi, A., 2003, Walker, I.D., 2005).

A comparison between IPMC, EAP and SMA is made. It is found that IPMC actuators can produce only 0.1–4.0 g of force depending on the thickness of the actuator (Kim, B., 2003), and the actuating voltage of EAP is as high as thousands volts (Walker, I.D., 2005). Obviously, these two actuators are not suitable. Though SMA has disadvantages of low actuating frequency and efficiency, it has advantages of large strain and stress, high energy density, low driven voltage and no noise, so SMA is the most suitable actuator for the bio-inspired suction cup. SMA actuators usually are wires and springs. Comparing wire with spring actuator at the same length, the spring actuator has a little smaller recovery force but much larger displacement, so SMA spring is chosen for actuating bio-inspired miniature suction cup to get larger volume change. SMA spring is divided into two-way and one-way shape memory effect spring by whether it can restore its original shape after heating. Two prototypes will be designed using two-way and one-way SMA spring respectively in section 3.

3. Bionic mechanism design

3.1. Bio-inspired miniature suction cup prototype 1

In section 2.1, biologic stalked suckers are considered to be suitable to engineering development. Imitating the piston structure of the stalked suckers, prototype 1 is designed. To decrease the volume of the prototype 1, a TWSME SMA spring is used because of no need of bias spring for the TWSME SMA spring. Fig.2 and Fig.3 are elementary and actual picture of the prototype 1. The prototype 1 has an outer and an inner cylinder fabricated by aluminous alloy. When the suction cup contacts with a substratum, there is a sealed air cavity among the two cylinders and the substratum. To keep the sealing of the the air cavity, an elastic sealing o-ring is set between two cylinders, and an elastic edge is bonded with the outer cylinder.

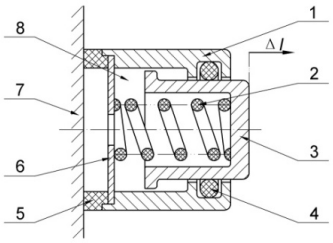

1-Outer cylinder 2-SMA actuator 3-Inner cylinder
4-O-ring 5-Elastic edge 6-Gasket 7- Substratum
8-Sealed air cavity

Fig. 2. Elementary figure of prototype 1

Fig. 3. Actual figure of prototype 1

If heated by an electrical current, austenitic phase transformation occurs in the TWSME SMA spring, and the spring begins to elongate and pushes the inner cylinder up relative to the outer cylinder, so the volume of the sealed air cavity is enlarged and negative pressure is generated. When cooled, the inner cylinder restores to its primitive position under the recovery force of the TWSME SMA spring, so the negative pressure is cancelled.

Because of an excellent cooling effect of aluminous alloy cylinders, the enlargement of the sealed air cavity can be seen as an isothermal process. According to the ideal gas law, the pressure difference ΔP generated by volume change ΔV can be derived as,

$$\Delta P = \frac{\Delta V}{\Delta V + V_0} P_0 \tag{1}$$

and,

$$\Delta V = \Delta l S \tag{2}$$

in euqations (1) and (2), P_0 denotes the atmospheric pressure. V_0 represents the original volume of the sealed air cavity. Δl is the elongation of the TWSME SMA spring. S is the effective suction area.

3.2. Bio-inspired miniature suction cup prototype 2

Because TWSME SMA spring is difficult to train, and a light overheating may make the spring lose two remembered geometries. Forces and maximum number of cycles are also limited comparing with the one way SMA spring. The prototype 2 actuated by an one way SMA spring with a bias is developed as showing in Fig. 4. Based on the conclusion of the section 2.1, main elements of the suction cup are SMA spring actuator, stiff margin, guiding element, leader and elastic element which can

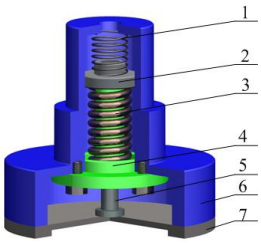

1-Bias spring 2- Gasket 3-SMA spring 4-Guiding element
5-Leader 6-Stiff margin 7- Elastic element

Fig. 4. Structure of bio-inspired suction cup prototype 2

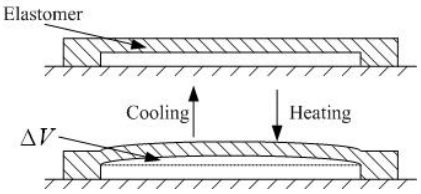

Fig. 5. The sealed air cavity in elastic element

surround an air cavity as showing in Fig.5. One end of the leader is bonded with the central point of elastic element, and the other end traverses through the guiding element and connects with the gasket through screw. The gasket can slip in the upper cylinder of the stiff margin. The outer circle of the elastic element is bonded with the circle of the stiff margin.

As showing in Fig.5, when the suction cup contacts with a substratum, the elastic element is clamped between the stiff margin and the substratum, and a sealed air cavity is formed. When heated by an electrical current, the SMA spring begins to elongate, and its one end pushes the leader. Because of the other end of the leader is bonded with the elastic element, so there is a deflection of the elastic element, and this leads to a deformation of the sealed air cavity, then a negative pressure is generated. When the heating current is broken, the SMA spring begins to cool naturally, and the bias spring pushes the leader back and negative pressure disappears. In the prototype 2, the stiff margin is also fabricated by aluminous alloy to quicken the cooling process, and the elastic element is made of silicone rubber with a Young's modulus of 1.5MPa. Silicone rubber is easy for deflecting and has a good sealing characteristic.

4. Analytical model of the prototype 2

In this section, the analytical model of prototype 2 will be developed to investigate the negative pressure response under different actuating currents. From the working principle of the prototype 2, it can be seen that the generation of the negative pressure accompanies with the electrical heating and phase transformation of the SMA spring, the deformation of the elastic element and the expanding of the sealed air cavity. It is a coupling process of various physical fields. The comprehensive model of the prototype 2 includes the electro-thermal model of heating SMA spring by Joule effect, the constitutive

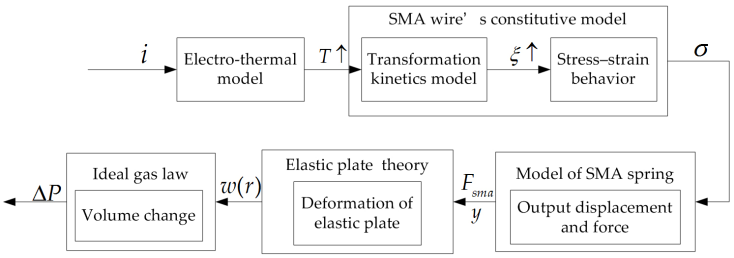

Fig. 6. Relationship between various models

Symbol	Meaning	Value
SMA		
ρ	Density(Kg/m^3)	6500
c_p	Specific heat(J/KgK)	320
R	Resistance(Ω)	0.15
h_0	Heat convection constant coefficient(W/m^{2}K)	120
h_2	Heat convection constant second order coefficient(W/m^{2}K^2)	0.001
T_∞	Ambient temperature(K)	293
D_M	Martensite Young modulus(Pa)	28e9
D_A	Austenite Young modulus(Pa)	75e9
ε_L	Initial stress	0.85%
μ_{sma}	Poisson's ration	0.33
M_s	Martensite start temperature(K)	313
M_f	Martensite finish temperature(K)	293
A_s	Austenitic start temperature(K)	313
A_f	Austenitic finish temperature(K)	333
C_M	Martensite curve fitting parameter(Pa/K)	10.3e6
C_A	Austenitic curve fitting parameter(Pa/K)	10.3e6
Θ	Thermal expansion factor(Pa/K)	0. 55e6
n	Number of turns	9
D	Coil diameter (mm)	7.3
d	Wire diameter (mm)	1.3
Elastic plate		
E_e	Young's modulus(Pa)	1.5e6
μ_e	Poisson's ration	0.45
h_e	Thickness(mm)	1.5
Sealed air cavity		
R_a	Radius(mm)	20
h_a	Thickness(mm)	1.5

Table 1. Definitions of symbols used in the model and values of material and geometrical parameters

model of SMA, the mechanical model to predict deformation of the elastic plate under compound load, and the thermo-dynamic model of the sealed air cavity. The relationship between various models is summarized in Fig.6. i, T, ξ, F_{sma} and y are actuating current, temperature, martensite fraction, output force and displacement of the SMA actuator respectively, and $w(r)$ is the deflection of the elastic element. Material and geometrical parameters, definitions of symbols used in the analytical model are given in Table 1. Next, each model will be built respectively.

4.1. Model of the SMA spring actuator

The model of the SMA spring actuator is made up of three parts: electro-thermal model, constitutive model and transformation kinetics model.

Electro-thermal analytical model of SMA proposes a system in thermal equilibrium in which heat transfer is uniformly distributed along materials surface. The main equation governing the relation between the input current i and the temperature $T(t)$ of SMA can be written as (Ikuta, K., 1991):

$$\rho c_p V \frac{dT(t)}{dt} = Ri^2(t) - hA(T(t) - T_\infty) \tag{3}$$

Where V, A are volume and surface area of the SMA actuator, and t is time variable. h is heat convection coefficient, which can be approximated by a second order polynomial of temperature to improve the electro-thermal model (Elahinia, M. H., 2002):

$$h = h_0 + h_2 T^2 \tag{4}$$

The non-linearity stress–strain behavior of SMA is caused by phase transformation from austenite phase to martensite phase or vice versa at different temperatures or stress. To describe the behavior, various constitutive models have been built, but the phenomenological model, which is developed by Tanaka (Tanaka, K., 1982), later modified by Liang and Rogers (Liang, C., 1990), and Brinson (Brinson, L.C., 1996), is used the most broadly.

In the constitutive model, the mechanical law governing the stress–strain behavior is,

$$\dot{\sigma} = D_{sma}\dot{\varepsilon} + \Theta\dot{T} + \Omega\dot{\xi} \tag{5}$$

$\Omega = -D_{sma}\varepsilon_L$ is the phase transformation contribution factor, and D_{sma} is the Young's modulus of SMA, who has a relationship with martensite fraction ξ $(0 \le \xi \le 1)$,

$$D_{sma} = \xi D_M + (1-\xi)D_A \tag{6}$$

For a quasi-static response of a bias spring SMA actuator in the suction cup, equation (5) can be integrated with respect to time,

$$\sigma - \sigma_0 = D_{sma}(\varepsilon - \varepsilon_0) + \Theta(T - T_0) + \Omega(\xi - \xi_0) \tag{7}$$

where variables with subscript "0" indicate initial conditions.

Because there are only shear stress τ and shear strain γ existing in SMA spring, equation (7) is not suitable. Basing on the multidimensional constitutive relation (Liang, C., 1992), equivalent shearing stress and strain $\sigma = \sqrt{3}\tau$, $\varepsilon = \sqrt{3}\gamma$, and shear modulus

$$G_{sma} = \frac{D_{sma}}{2(1+\mu_{sma})} \tag{8}$$

are introduced to equation (7) and given,

$$\tau - \tau_0 = G(\gamma - \gamma_0) + \frac{\Theta}{\sqrt{3}}(T - T_0) + \frac{\Omega}{\sqrt{3}}(\xi - \xi_0) \tag{9}$$

Considering the design principle of conventional springs, a general form of the force (F_{sma})-displacement (y)-temperature (T)-martensite fraction (ξ) relation of SMA springs may be derived as (Liang, C., 1997),

$$F_{sma} = \frac{d^4 G_{sma}}{8nD^3} y + \frac{\pi d^3 \Omega}{8\sqrt{3}D}(\xi - \xi_0) + \frac{\pi d^3 \Theta}{8\sqrt{3}D}(T - T_0) \tag{10}$$

In equation (10), martensite fraction ξ is changed along with temperature. There is a transformation kinetics model which describes the phase transformation process. The heating of SMA results in reverse transformation from martensite to austenite when temperature is $A_s \le T \le A_f$, and

$$\xi = \frac{\xi_M}{2}\{\cos[a_A(T - A_s) + b_A\sigma_{eff}] + 1\} \tag{11}$$

The cooling of SMA results in forward transformation from austenite to martensite when temperature is $M_f \le T \le M_s$, and

$$\xi = \frac{1-\xi_A}{2}\cos[a_M(T - M_f) + b_M\sigma_{eff}] + \frac{1+\xi_A}{2} \tag{12}$$

Where ξ_M and ξ_A are martensite fractions at the beginning of the reverse and forward transformation respectively. In equations (11) and (12), $a_M = \pi/(M_s - M_f)$, $b_M = -a_M / C_M$, $a_A = \pi/(A_f - A_s)$, $b_A = -a_A / C_A$. σ_{eff} is effective stress in the case of spring actuator, and it has a relationship with F_{sma} (Liang, C., 1997).

$$\sigma_{eff} = \frac{8\sqrt{3}D}{\pi d^3} F_{sma} \tag{13}$$

4.2. Deformation of the elastic element

To establish the mechanical model of the elastic element, first force analysis is made when the suction cup adheres. In Fig 7, F_{sma} is the pulling force of the actuator through the leader, which causes the deformation of the elastic element. N_1, N_1 and F_b are constrained force given by substratum and the stiff margin, and ΔPS is the negative pressure suction force. The rim of the elastic element can be seen as static because it is bonded with the stiff

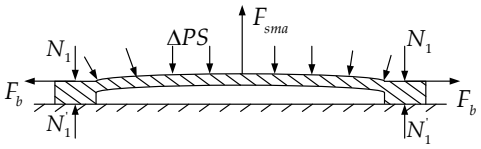

Fig. 7. Force analysis of elastic element

margin, so the deformation of the elastic element can be seen as a problem of clamped thin circular plate subjected to the combined action of a uniform lateral pressure (ΔP) and a concentrated central load (F_{sma}).

Some hypothesizes are made to simplify the problem. First, the material non-linearity of the elastic plate is not considered, which means that the elastic plate is seen as isotropy linear elasticity. Second, F_{sma} is seen as a concentrated central load. Using von Karman equation, the deformation of the thin circular plate subjected to the combined action of uniform lateral pressure and a concentrated central load can be sovled by following equations (Hwang, C., 1982),

$$\begin{cases} D_e \dfrac{d}{dr}\dfrac{1}{r}\dfrac{d}{dr} r \dfrac{dw(r)}{dr} = N_r \dfrac{dw(r)}{dr} + \dfrac{\Delta P r}{2} - \dfrac{F_{sma}}{2\pi r} \\ r\dfrac{d}{dr}\dfrac{1}{r}\dfrac{d}{dr}(r^2 N_r) = -\dfrac{E_e h_e}{2}\left(\dfrac{dw(r)}{dr}\right)^2 \\ N_i = \dfrac{d}{dr}(rN_r) \end{cases} \tag{14}$$

where $D_e = \dfrac{E_e h_e^{\,3}}{12(1-\mu_e^{\,2})}$ is flexural rigidity. N_r and N_i are membrane forces on neutral layer. $w(r)$ is the deflection function, and r is polar coordinate. Boundary conditions are:

When $r = R_a$,

$$w = 0,\ \frac{dw(r)}{dr} = 0,\ (1-\mu_1)N_r + r\frac{dN_r}{dr} = 0 \tag{15}$$

When $r = 0$, $\dfrac{dw}{dr}$ and N_r is finite.

Because it is difficult to solve the nonlinearity coupling equation (14), a effective stiffness is used to solve the central displacement Δd of the elastic element (Yina, H.L., 2007). From force analysis in Fig.7, it is obvious that,

$$\Delta d = \frac{F_{sma} - \Delta PS - kx}{k_{eff}} \tag{16}$$

Where k and x are stiffness and displacement os the bias spring; k_{eff} denotes the effective stiffness of the elastic element and it has a relationship with the elastic element's thickness h_e and radius R_a (Ugural, A.C., 1999),

$$K_{eff} = \frac{E_e h_e^3}{0.01491(1-\mu_e^2)R_a^2} \tag{17}$$

also there is a constraint condition that

$$y = \Delta d \tag{18}$$

where y is the displacement of the SMA spring.

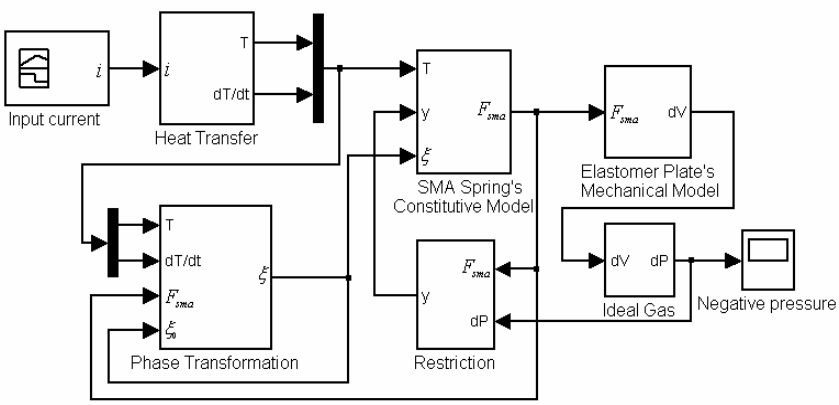

Fig. 8. Matlab/simulink block diagram of prototype 2

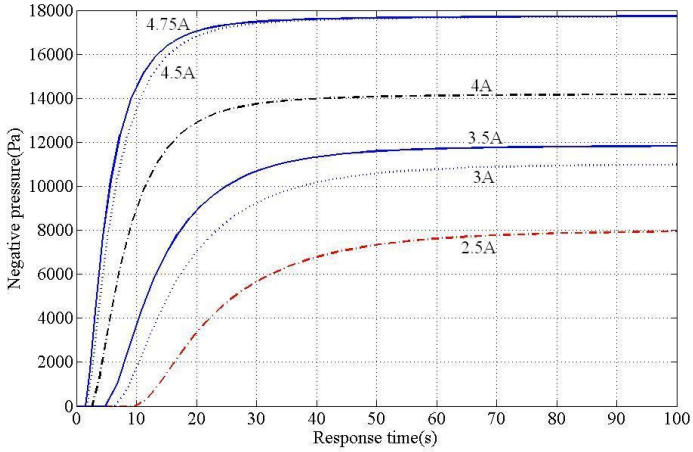

Fig 9. Simulation results of negative pressure response

4.3 Sealed air cavity

Air sealed in the cavity can be seen as ideal gas in adiabatic condition. Using ideal gas law, the negative pressure ΔP generated by the volume change ΔV can be derived as,

$$\Delta P = \frac{\Delta V}{V_0 + \Delta V} P_0 \tag{19}$$

The volume change ΔV is a function of the deflection of the elastic element Δd, and it can be expressed as (Yina, H.L., 2007),

$$\Delta V = \Delta d \int_0^{R_a} \int_0^{2\pi} (1 - \cos\frac{\pi r \cos\theta}{R_a})(1 - \cos\frac{\pi r \sin\theta}{R_a}) dr d\theta \tag{20}$$

For a given electrical current i, through equations (3)-(13), the force-displacement-temperature relation of the SMA spring actuator can be calculated. Plusing equations (16)-(20), negative pressure ΔP is determined and it should be a function of given current i. Based on the above analysis, all models have been programmed and linked together in matlab/simulink platform to simulate the negative pressure response as showing in Fig.8. Values of parameters in the model are in table 1 and simulation results are in Fig.9. It is obvious that the negative pressure increases, and the response time decreases with an increasing of the actuating currents.

5. Experiments

In order to heat the SMA actuators, a constant current source is used to supply power. In prototype 1, the TWSME extension TiNi spring has an outer diameter of 9 mm, wire diameter of 1.3 mm and effective turns of 9. The prototype 1 has an outer diameter of 28mm, height of 25mm and weight of 30g. Experiments indicate that the prototype 1 can lift as weighty as 200g (Fig.10), but it is difficult to cancel negative pressure because of large friction force between the sealing o-ring and the inner cylinder and small recoveing force of TWSME spring.

To get the negative pressure response in the sealed cavity of prototype 2, a pressure sensor MPX5100, which has a measure range of 100 kPa and a full scale voltage of 5v is used. Because an absolute sealing of the sealed air cavity is impossible, to measure more exactly, the pressure

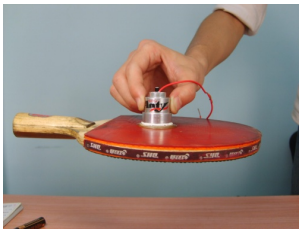

Fig. 10. Prototype 1's suction experiment

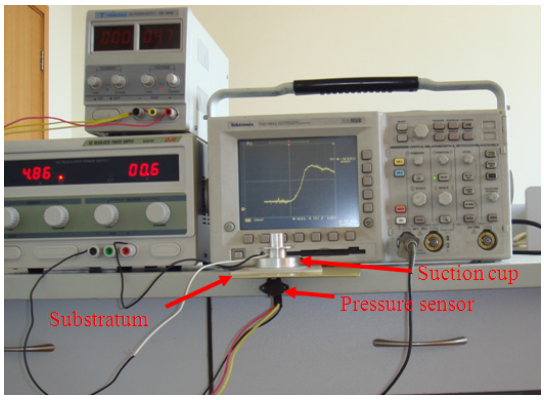

Fig. 11. Experiment of measuring negative pressure response of prototype 2

sensor, which is fixed on the bottom surface of the substratum (Fig.11), connects with the sealed air cavity in the prototype 2 through a hole on the substratum. A thin layer of rubber, which can reduce leakage of the sealed air cavity, is bonded with the top surface of the substratum. The whole experiment equipments are in Fig.11. Parameters of the prototype 2 are in table 1. The weight of the whole suction cup is about 50g.

Fig.12 is the negative pressure response curve under a constant driving current of 4A. We can see that after 35 seconds heating, negative pressure reaches to the highest (about 12000Pa) and it maintains this value. The reason is that the SMA spring achieves to a constant temperature which makes the spring in a thermal equilibrium state, and the displacement and output force of the spring cannot become larger at this time, so the negative pressure reaches to the largest. If the sealing condition is ideal, the negative pressure will drop slowly and can maintain for a long time.

The negative pressure can get at different actuating currents shows in Fig.13. When the actuating current is small, there is not negative pressure because the temperature of SMA spring is lower than the austenitic phase transformation starting temperature. When the actuating current is larger than 1.5A, austenitic phase transformation begins, and a larger current means a higher temperature and a larger output force, so a bigger

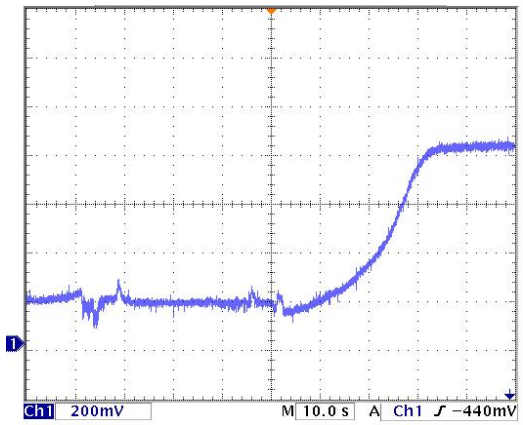

Fig. 12. Negative pressure response of prototype 2 under actuating current of 4A

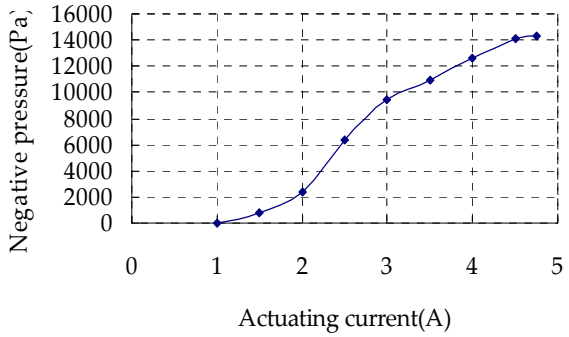

Fig. 13. Maximal negative pressure at different actuating currents of prototype 2

volume change is gotten, and the negative pressure is larger. When the current is larger than 4.5A, the SMA spring elongates fully and the negative pressure comes to the largest which is about 14000 Pa.

Negative pressure response time is the time interval that negative pressure from zero reaches to the largest under a constant actuating current. The response time under different actuating currents is shown in Fig.14. It can be seen that the response time decreases with an increasing of the actuating current. At an actuating current of 4.75A, the response time needs 20s.

Comparing Fig.9 with Fig.13 and Fig.14, simulation results accord with experiments approximately, but there is an obvious error especially in the negative pressure. This is because that the actuating force of the SMA spring cannot be simplified as a concentrated force, and this operation will overestimate the deflection of the elastic element as well as the generated negative pressure because of stress centralization. The material nonlinearity of the elastic element and the leakage of sealed air cavity also have responsibility for the overestimate.

Because wall climbing robots usually work on a vertical wall, the suction characteristics of prototype 2 under load whose action direction is parallel with vertical substratum are tested at an actuating current of 4A (Fig. 15). Because there is a leakage all the time, at first suction maintaining time is defined to describe the time that the suction cup can hold a load. The suction maintaining time

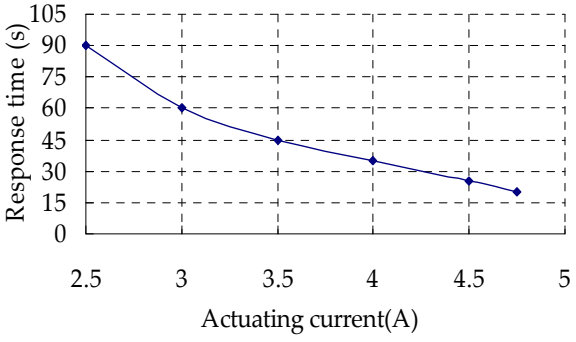

Fig. 14. Relation of response time and actuating current of prototype 2

Fig. 15. The prototype 2 under vertical load

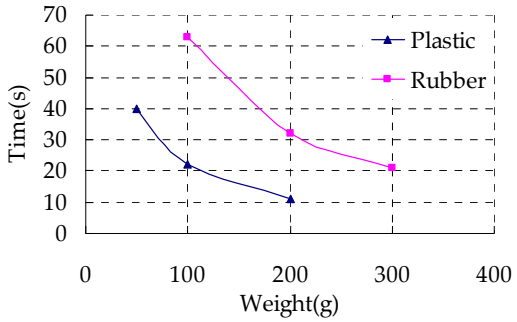

Fig. 16. Suction maintaining time at different loads and substratums of prototype 2

is from the time that negative pressure increases to the largest value that makes the suction cup to hold the load, to the time that the suction cup can not hold the load because of an air leakage. Experiments show that the suction maintaining time has a relationship with the material of substratum and the load weight (Fig.16). When the substratum is a flat rubber surface, the suction cup can catch up heavier load for a longer time, which is caused by a better sealing condition and a larger friction coefficient of rubber surface. Experiments show that the prototype 2 can hold a load whose weight is 200g for 32s on flat rubber surface.

Comparing the two bio-inspired miniature suction cups, they are actuated by TWSME spring and one way SMA spring with a bias respectively, and they all can hold a load weight 200g successfully, which is about several times of their own weight. The prototype 1 has a smaller volume and a lighter weight than the prototype 2, but there is not a dynamic o-ring and structures of inner and outer cylinder, so the prototype 2 can detach or attach to substratum more freely.

6. Conclusion and future work

Two prototypes of bio-inspired miniature suction cup actuated by SMA spring actuators are developed. Prototype 1 with a TWSME spring actuator which imitate piston structure of stalked suckers is designed first, and its dimension can be reduced to a few centimeters and the weight is just 30g, but it can lift a load weight 200g, the disadvantages of the prototype 1 are that it can not cancel the negative pressure because of the actuator's small recovery force and firction force between inner cylinder and sealing ring. The weight of prototype 2 is 50g, who has a main structure of SMA spring actuator, stiff margin, guiding element, leader and elastic element, and it is designed based on studying common grounds of biologic suction apparatus to avoid disadvantages of the first prototype. The second prototype's analytical model is founded considering SMA's constitutive model, thin elastomer plate's deflection under compound load and thermo-dynamic model of sealed air cavity. The analytical model is simulated on matlab/simulink platform. At last, experiments are done to validate the analytical model. At an actuating current of 4A, the second prototype's highest negative pressure can reach 12000Pa, and it can hold a vertical load weight 200g for 32s on flat rubber surface. Comparing with the traditional suction cup, this kind of bio-inspired miniature negative pressure suction cup actuated by SMA does not need any air pumps, and it also has advantages of no noise, little volume and weight, so it can be used as a suction mechanism for miniature wall climbing robots.

Future improvements of the bio-inspired miniature suction cup are planned in the following two aspects: first is to make the negative pressure respond more quickly by using SMA wire or film actuators, and adopting some fast control methods. Second is to improve the structure of bio-inspired suction cup. For example, embed SMA actuators into the elastic element; apply nanomolding technology to fabricate elastic edge as suckers of octopus to improve sealing and so on.

7. Acknowledgments

The support of the National Science and Technology Foundation of China, through NSTF Grant No. 60675052, is gratefully acknowledged.

8. References

Asbeck, A.T.; Kim, S.; Cutkosky, M.R.; Provancher, W.R. & Lanzetta,M. (2006). Scaling Hard Vertical Surfaces with Compliant Microspine Arrays. *The International Journal of Robotics Research*, Vol.25, NO. 12, pp.1165-1179, 0278-3649

Autumn, K. & Peattie, A. (2002). Mechanisms of adhesion in geckos. *Integrative and Comparative Biology*, Vol.42, No.6, pp. 1080-1090, 1540-7063

Bandyopadhyay, P.R.; Hrubes, J.D. & Leinhos, H.A. (2008). Biorobotic adhesion in water using suction cups. *Bioinspiration and Biomimetics*, Vol.3, No.1, pp. 16003, 1748-3190

Brinson, L.C.; Bekker, A. & Hwang, S. (1996). Deformation of shape memory alloys due to thermo-induced transformation. *Journal of Intelligent Material Systems and Structures*, Vol.7, No.1, pp. 97-107, 1530-8138

Chan, B.; Ji, S.; Koveal, C. & Hosoi, A.E. (2007). Mechanical Devices for Snail-like Locomotion. *Journal*

of Intelligent Material Systems and Structures, Vol.18, No.2, pp.111-116, 1045-389X

Dai, Z.D.; Gorb, S.N. & Schwarz, U. (2002). Roughness-dependent friction force of the tarsal claw system in the beetle pachnoda marginata(coleoptera, scarabaeidae). *Journal of Experimental Biology*, Vol.205, No.16, pp. 2479-2488, 0022-0949

Dean, M., & Girish, D. (2005). Design, fabrication and testing of a smart robotic foot, *Robotics and Autonomous Systems*, Vol.51, No.2-3, pp.207-214, 0921-8890

Dixon, A.F.G.; Croghan, P.C. & Gowing, R.P. (1990). The Mechanism by Which Aphids Adhere to Smooth Surfaces. *Journal of Experimental Biology,*, Vol.152, pp.243-253, 0022-0949

Elahinia, M. H. & Ashrafiuon, H. (2002). Nonlinear control of a shape memory alloy actuated manipulator. *Journal of Vibration & Acoustics – Transactions of the ASME*, Vol. 124, No.4, pp. 566-575, 1048-9002

Ellem, K.G.; Furst, J.E. & Zimmerman, k.D. (2002). Shell clamping behaviour in the limpet Cellana tramoserica. *The Journal of Experimental Biology*, Vol.205, No.4, pp. 539-547, 0022-0949

Fulcher, B. A. & Motta, P. J. (2006). Suction disk performance of echeneid fishes. *Canadian Journal of Zoology*, Vol.84, No.1, pp. 42-50, 0008-4301

Grasso, W.F. & Setlur, P. (2007). Inspiration, simulation and design for smart robot manipulators from the sucker actuation mechanism of cephalopods. *Bioinspiration and Biomimetics*, Vol.2, No.4, pp.S170-S181, 1748-3190

Gray, J.; Lissmann, H.W. & Pumphrey, R.J. (1938). The Mechanism of Locomotion in the Leech(Hirudo Medicinalis Ray). *Journal of Experimental Biology*, Vol.15, pp.408-430, 0022-0949

Hwang, C. (1982). Large deflection of circular plate under compound load. *Applied Mathematics and Mechanics*, Vol.4, No.5, pp. 791-804, 0253-4827

Ikuta, K.; Tsukamoto, M. & Hirose, S. (1991). Mathematical model and experimental verification of shape memoryalloy for designing micro actuator, Proceedings of the IEEE Micro Electro Mechanical Systems Conference, pp. 103-108, 0-87942-641-1, Nara, Japan, January 1991

Kim, B.; Ryu, J.; Jeong, Y.; Tak, Y.; Kim, B.; Park, J.O. (2003). A ciliary based 8-legged walking micro robot using cast IPMC actuators, Proceedings of the IEEE International Conference on Robotics and Automation, pp. 2940–2945, 1050-4729, Taipei, September, 2003

Liang, C. & Rogers, C.A. (1990). One-Dimensional Thermomechanical Constitutive Relations for Shape Memory Materials. *Journal of Intelligent Material Systems and Structures*, Vol.1, No.2, pp. 207-234, 1530-8138

Liang, C. & Rogers, C.A. (1992). A Multi-Dimensional Constitutive Model for Shape Memory Alloys. *Journal of Engineering Mathematics*, Vol.26, No.3, pp. 429-443, 0022-0833

Liang, C. & Rogers, C.A. (1997). Design of shape memory alloy springs with application in vibration control. *Journal of Intelligent Material Systems and Structures*, Vol.8, No.4, pp. 314-322, 1530-8138

Menciassi, A. & Dario, P. (2003). Bio-Inspired Solutions for Locomotion in the Gastrointestinal Tract: Background and Perspectives. *Philosophical Transactions: Mathematical, Physical and Engineering Sciences*, Vol.361, No.1811, pp. 2287-2298, 1364503X

Nachtigall, W. (2005). Animal attachments: Minute, manifold devices. Biological variety — Basic physical mechanisms — A challenge for biomimicking technical stickers, *Bionik*, pp. 90-122, Springer Berlin Heidelberg, 978-3-540-21890-6

Persson, B.N.J. (2007). Wet adhesion with application to tree frog adhesive toe pads and tires. *Journal of Physics: Condensed Matter*, Vol.19, No.37, pp.376110-376126, 0953-8984

Riskin, D.K. & Fenton, M.B. (2001). Sticking ability in Spix's disk-winged bat, Thyroptera tricolor (Microchiroptera: Thyropteridae). *Canadian Journal of Zoology*, Vol.79, No.12, pp. 2261-2267, 0008-4301

Smith, A.M. (1996). Cephalopod Sucker design and the Physical Limits to Negative Pressure. *Journal of Experimental Biology*, Vol.199, No.4, pp. 949-958, 0022-0949

Sitti, M. & Fearing, R.S. (2003). Synthetic Gecko Foot-Hair Micro/Nanostructures as Dry Adhesives. *Journal of Adhesion Science and Technology*, Vol.17, No.5, pp. 1055-1073, 1568-5616

Tanaka, K. & Nagaki, S. (1982). A thermomechanical description of material with internal variables in the process of phase transformation. *Archive of Applied Mechanics (Ingenieur Archiv)*, Vol.51, No.5, pp. 287-299, 0939-1533

Ugural, A.C. (1999). *Stresses in Plates And Shells*, McGraw-Hill, 0070657696, Boston

Walker, I.D., Dawson, D.M., Flash, T., Grasso, F.W., Hanlon, R.T., Hochner, B., Kier, W.M., Pagano, C.C., Rahn, C.D. and Zhang, Q.M. (2005). Continuum Robot Arms Inspired by Cephalopods, Proceedings of SPIE, Gerhart, G.R.; Shoemaker, C.M. & Gage, D.W., Vol. 5804, pp. 303-314

Werner, B. & Florian, M. (2005). Climbing Without a Vacuum Pump, Proceedings of the 7th International Conference CLAWAR, pp. 935-942, 978-3-540-22992-6, Madrid, Spain, September, 2004, Springer Berlin Heidelberg

William, M.K., & Andrew, M.S. (2002). The Structure and Adhesive Mechanism of Octopus Suckers. *Integrative and Comparative Biology*, Vol.42, No.6, pp.1146-1153, 1540-7063

Xu, Z.L. & Ma, P.S. (2006). A wall-climbing robot for labeling scale of oil tank's volume. *Robotica*, Vol.20, pp.209-212, 0263-5747

Yina, H.L.; Huangb, Y.C.; Fangb, w. & Hsieh, J. (2007). A novel electromagnetic elastomer membrane actuator with a semi-embedded coil. *Sensors and Actuators A: Physical*, Vol.139, No.1-2, , pp. 194-202, 0924-4247

Zhao, Y.Z. ; Fu, Z.; Cao, Q.X. & Wang, Y. (2004). Development and applications of wall-climbing robots with a single suction cup, *Robotica*, Vol.22, pp.643-648, 0263-5747

Zhu, T., Liu, R.; Wang, X.D. & Wang, K. (2006). Principle and Application of Vibrating Suction Method, IEEE International Conference on Robotics and Biomimetics, pp. 491-495, 1-4244-0571-8, Kunming, China, December, 2006